Inverse Energy Cascade Correlated with Turbulent-Structure Generation in Toroidal Plasma

H. Xia* and M. G. Shats†

Plasma Research Laboratory, Research School of Physical Sciences and Engineering, Australian National University, Canberra ACT 0200, Australia

(Received 29 August 2002; revised manuscript received 8 August 2003; published 6 October 2003)

We report the first experimental observation of the inverse energy cascade correlated with the generation of large turbulent structures. Spectral energy is nonlinearly transferred from the unstable region of the spectrum into large coherent structures and into broadband turbulence in agreement with theoretical expectations. These results are obtained by producing plasma in the H-1 heliac whose parameters allow a single-field, Hasegawa-Mima–type model to be used for the spectral energy transfer analysis.

DOI: 10.1103/PhysRevLett.91.155001 PACS numbers: 52.35.Ra, 52.30.–q, 52.35.Mw, 52.55.Hc

Plasma turbulence, which is believed to be one of the key components which determines the plasma behavior, is often characterized by broad fluctuation spectra whose maxima are observed at the longest measured scales [1]. Since waves, which become unstable and eventually generate a turbulent spectrum are initially unstable only in a limited spectral range, a nonlinear mechanism of the wave-wave interaction in the plasma is necessary to explain observations. Such a mechanism, namely, three-wave interactions leading to the energy cascade, has been suggested for the two-dimensional turbulence [2] and the magnetized plasma [3]. In some conditions the "inverse cascade," or the nonlinear spectral energy transfer towards lower wave numbers, has been predicted. The spectral energy can condensate due to the inverse cascade in large coherent structures, such as, for example, vortex structures (for review, see [4]) and zonal flows [5]. However, no experimental results are available that verify the role of the inverse cascade in the generation of broadband spectrum. The estimation of the nonlinear energy transfer in the fluctuation spectrum is one of the main problems. A technique for a quantitative estimation of the energy cascade between waves in turbulent plasma has been developed by Ritz *et al.* [6,7] and has been applied to the data from the Texas Experimental Tokamak (TEXT) edge turbulence. This model is suitable for studying the spectral dynamics in single-field turbulence, such as neutral fluid turbulence, or the Hasegawa-Mima turbulence in plasma [8]. Later an extended version of this technique was proposed by Kim *et al.* [9] and it has been applied to the Tokamak Fusion Test Reactor (TFTR) plasma core fluctuations. In both TEXT and TFTR no strong cascade of the fluctuation power to lower wave numbers has been found. One difficulty might have been that the Hasegawa-Mima–type turbulence is not very commonly observed in fusion research plasma experiments. Crossley *et al.* [10] have proposed the "amplitude correlation" technique and have found evidence of the inverse cascade in the fluctuation spectra of the UMIST (University of Manchester Institute of Science and Technology) quadrupole plasma device. In this work, however, no broadband spectra have been observed.

In this Letter we report the first experimental evidence of the inverse energy cascade which results in the generation of the broadband spectrum and large-scale turbulent structures such as zonal flow in the toroidal plasma. Such a condensation of the spectral energy has been theoretically predicted by Hasegawa *et al.* [3]. Our results on the spectral power transfer based on the extended Ritz model are correlated with this prediction and also agree with the expected shape of the broadband turbulent spectrum.

We present the analysis of results obtained in the H-1 toroidal heliac [11] (major radius of $R = 1$ m and mean minor plasma radius of about $\langle a \rangle \approx 0.2$ m) under the following plasma conditions (see, for example, [12] and references therein): $n = 1 \times 10^{18}$ m^{-3}, $T_e \sim 10$ eV, $T_i \sim 40$ eV in argon at a filling pressure of $(1–4) \times 10^{-5}$ Torr and at low magnetic fields, $B = (0.05–0.12)$ T. Such plasma is produced by ~60 kW of the radio-frequency waves at 7 MHz. Various combinations of electric probes are used to characterize plasma parameters, as described in detail in [13]. We analyze fluctuations in the floating potential, V_f, rather than the plasma potential to achieve the best signal-to-noise ratio to which the higher-order spectral analysis is very sensitive. The amplitude and the phase spectra of electron temperature fluctuations in our conditions are found to be identical to those in the floating potential. Therefore this simplification does not affect our results.

Strong fluctuations in electron density ($\tilde{n}/n \sim 0.25$) and in electrostatic potential are observed in the H-1 plasma at low magnetic fields ($B < 0.1$ T) [14]. An identification of these fluctuations is not certain, but we have found several signatures of resistive pressure gradient driven instability [14]. A frequency power spectrum of the V_f fluctuations in the low confinement mode is presented in Fig. 1(a). The spectrum decays exponentially up to $f \sim 80$ kHz showing several quasicoherent features in the frequency range of $f < 20$ kHz.

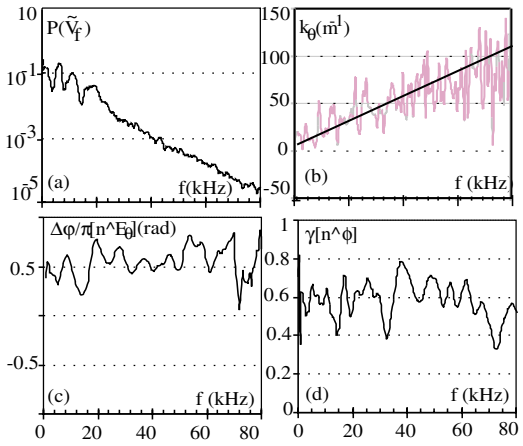

FIG. 1 (color online). (a) Power spectrum of the fluctuations in the floating potentials, V_f, at $r/a = 0.5$, $B = 0.046$ T, $P_{\mathrm{rf}} = 55$ kW; spectra of (b) the measured poloidal wave number spectrum $k_\theta(f)$; (c) the phase shift between fluctuations in the electron density, $\tilde{n}_e$, and poloidal electric field, $\tilde{E}_\theta$; and (d) the coherence between fluctuations in the electron density, $\tilde{n}_e$, and the floating potential, $\tilde{V}_f$.

The mode coupling mechanism in the turbulence may arise from the $\mathbf{E} \times \mathbf{B}$ convection of the density fluctuations [15] or from the polarization drift [8] which appear in the equation of the ion dynamics [16]:

$$\partial n_i/\partial t + \mathbf{V}_E \cdot \nabla n_i + \nabla \cdot (n_i \mathbf{V}_P) = 0. \tag{1}$$

Here $\mathbf{V}_E$ and $\mathbf{V}_P$ are the fluctuating $\mathbf{E} \times \mathbf{B}$ and the polarization drift velocities correspondingly and $n_i = n_0 + \tilde{n}_i$ consists of mean and fluctuating parts. The $\mathbf{E} \times \mathbf{B}$ nonlinearity arises from the $\mathbf{V}_E \cdot \nabla \tilde{n}_i$ term, while the polarization drift nonlinearity originates from the $n_0 \nabla \cdot \mathbf{V}_P$ term. The electron density fluctuations are considered as a sum of the adiabatic (Boltzmann) and nonadiabatic parts: $\tilde{n}_e = n_0 \exp(e\tilde{\phi}/T) + \delta n_e$. If $\delta n_e = 0$ the problem can be reduced to a single-field model by substituting $\tilde{n}_i = \tilde{n}_e$ in Eq. (1) and rewriting it for the potential fluctuations $\tilde{\phi}$. In other words, when $\delta n_e = 0$, $\tilde{\phi}$ and $\tilde{n}_e$ should be in phase. This would also mean no turbulent transport, $\Gamma_{\mathrm{turb}} = \langle \tilde{n}_e \tilde{E}_\theta / B_T \rangle = 0$, because $\tilde{n}_e$ and the poloidal electric field fluctuations $\tilde{E}_\theta$ would have a $\pi/2$ phase shift ($\tilde{E}_\theta = -\nabla_\theta \tilde{\phi}$). The adiabatic electron response should also indicate that the polarization drift dominates over $\mathbf{E} \times \mathbf{B}$ drift nonlinearity. It has been shown in [17] that the former dominates at large $k_\perp \rho_s$ (where $k_\perp$ is the perpendicular wave number and ρ_s is the ion gyroradius at the electron temperature), while the latter is dominant at small $k_\perp \rho_s$. The two nonlinearities are approximately equal when $k_\perp \rho_s = \delta = c_s/(L_n \nu_e)$. Here c_s is the ion acoustic velocity, L_n is the density scale length, and ν_e is the electron collision rate. In our experiment $k_\perp \rho_s (= 0.5\text{–}2.5) \gg \delta (\approx 0.1)$ due to the large ion mass (argon), low magnetic field, and high collisionality. Thus we expect the polarization drift to dominate over $\mathbf{E} \times \mathbf{B}$ drift nonlinearity. This correlates with our measurements of the phase shift between $\tilde{n}_e$ and $\tilde{E}_\theta$ shown in Fig. 1(c). This phase shift is close to $\pi/2$ over the entire spectrum suggesting the adiabatic electron response. We also find that the density and potential fluctuations are well correlated in the spectral range of interest. Figure 1(d) shows that the coherence between $\tilde{n}_e$ and $\tilde{\phi}$ is about 0.6 over a broad spectral range, also confirming our conclusion about adiabatic electron response.

Summarizing, the above results and estimates justify using a single-field model proposed by Ritz *et al.* [7] to analyze the spectral power transfer in the H-1 turbulence.

In the model, the change in the spectrum is due to the linear growth rate γ_k, the dispersion ω_k, and the wave-wave coupling coefficient Λ_{k_1,k_2}, as

$$\frac{\partial \phi_k(t)}{\partial t} = (\gamma_k + i\omega_k)\phi_k(t) + \sum_{k=k_1+k_2} \Lambda_{k_1,k_2} \phi_{k_1}(t) \phi_{k_2}(t), \tag{2}$$

where $\phi(x, t) = \sum_k \phi_k(t) e^{i\vec{\mathrm{k}} \cdot \vec{\mathrm{x}}}$. The wave kinetic equation with the spectral power $P_k = \phi_k(t)\phi_k^*(t)$ (asterisk denotes complex conjugate) can then be written as

$$\partial P_k/\partial t \approx \gamma_k P_k + \sum_{k=k_1+k_2} T_k(k_1, k_2), \tag{3}$$

where $T_k(k_1, k_2)$ is the nonlinear power transfer function (PTF), which quantifies the energy exchanged between different waves in the spectrum due to three-wave interactions. By redefining $X_k = \phi(k, t)$ and $Y_k = \phi(k, t + \tau)$, one can obtain a simple turbulent model from Eq. (2) with a single input and single output with the linear and quadratic couplings [7]:

$$Y_k = L_k X_k + \sum_{k=k_1+k_2} Q_k(k_1, k_2) X_{k_1} X_{k_2}. \tag{4}$$

Here, Y_k and X_k are the Fourier transforms of the measured output and input signals and L_k and $Q_k^{k_1,k_2}$ are the linear and nonlinear coupling coefficients correspondingly.

To determine the coupling coefficients L_k and $Q_k^{k_1,k_2}$ in Eq. (4) and eventually the linear growth rate γ_k and the PTF $T_k(k_1, k_2)$ of Eq. (3), statistically averaged estimations of the autopower spectrum $\langle X_k X_k^* \rangle$, cross-power spectrum $\langle Y_k X_k^* \rangle$, autobispectrum $\langle X_k X_{k_1}^* X_{k_2}^* \rangle$, cross bispectrum $\langle Y_k X_{k_1}^* X_{k_2}^* \rangle$, and the fourth order moment $\langle X_{k_1} X_{k_2} X_{k'_1}^* X_{k'_2}^* \rangle$ are needed. In the original model [6] the fourth order moment is approximated by the square of the second-order moment. In the modified method [18], stationarity of the turbulence is enforced, and the fourth order moment is retained. Both techniques have been tested with our experimental data, showing the qualitative agreement. All results presented here are obtained by retaining the fourth order moments.

In the model, the k domain is transformed into the frequency domain, so that the three-wave interactions obey the frequency selection rule, $f = f_1 + f_2$. This transformation can be justified by the measurement of the wave number spectrum.

Wave numbers of the fluctuations have been measured using two poloidally separated probes as $k_\theta = \Delta\varphi/\Delta y$, where $\Delta\varphi$ is the phase shift. This has been analyzed in the frequency domain and the $k_\theta(f)$ dependence is shown in Fig. 1(b) by the grey line. This dependence has a linear trend; however, a large ripple is usually observed. This ripple can be reduced by statistical averaging over a large number of realizations. Its origin is currently under investigation. The amplitude of the ripple correlates with the relative strengths of coherent structures to the level of broadband fluctuations. Zonal flows are commonly observed among the structures [12]. It has been shown recently [19] that in the presence of zonal flows phases of potential fluctuations become more random, which could therefore affect the $k_\theta(f)$ measurements. The linear approximation of the dispersion is shown in Fig. 1(b) by the black line. The fluctuations' phase velocity derived from this linear dispersion agrees within 10% with the measured $\mathbf{E} \times \mathbf{B}$ drift velocity in these discharges.

Spectra are estimated by ensemble averaging over many independent realizations. This averaging is essential for the statistical error of the higher-order cumulant estimation to be small. Floating potential signals are digitized at 0.3 MHz with the typical plasma pulse length of ~(60–80) ms. The signals are then divided into 600 segments, so that each segment contains 60 data points. Such a severe statistical averaging results in the reduced frequency resolution of the spectra of the PTF, $\Delta f \sim$ (4–5) kHz. Considering the large amount of averaging needed to obtain the linear $k_\theta(f)$ dependence, we may suggest that the averaging needed for PTF estimation is not just a numerical effect but is dictated by the need to satisfy the model assumption about the $k_\theta(f)$ linearity.

Results of the spectral power transfer estimations are shown in Fig. 2 for two plasma confinement modes in H-1, namely, the L and the H mode [14]. Plasma transits spontaneously from the L to the H mode within ~1 ms. The transition is accompanied by the fluctuation suppression and the onset of the strongly sheared radial electric field, E_r. The turbulence spectrum is strongly altered across the transition. Shown in Figs. 2(a) and 2(b) are the power spectra at low (~ 4 kHz) and high frequency resolution (~ 0.6 kHz), respectively. The fluctuation level is reduced across the L-H transition over the entire spectrum except $f \sim 40$ kHz. The energy stored in the electrostatic fluctuations ϕ_k can be written as [3] $W_k = (1 + k_\perp^2)|\phi_k|^2$. The nonlinear energy transfer function $W_{\mathrm{NL}}^k = (1 + k_\perp^2)\sum_k T_{k_1,k_2}$ is shown in Fig. 2(c). In the L mode W_{NL}^k is negative in the broadband spectral region of $f =$ (20–60) kHz suggesting that on average waves in

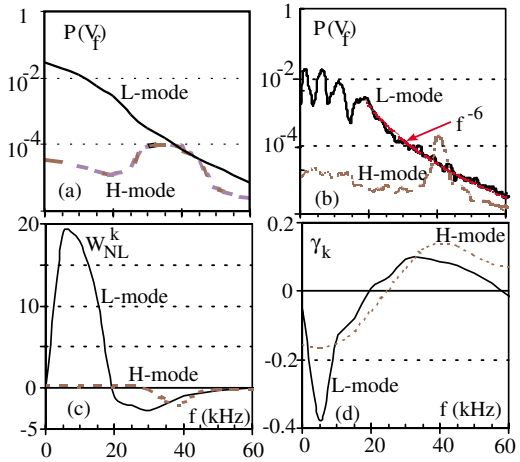

FIG. 2 (color online). Power spectra of the floating potential fluctuations in L (solid lines) and H (dashed lines) modes at (a) frequency resolution of 4 kHz and (b) frequency resolution of 0.6 kHz, and the power law fit $P \sim f^{-6}$ to the L mode spectrum. (c) The nonlinear (NL) energy transfer function W_{NL}^k in the L and H modes. (d) The linear growth rate γ_k derived from Eq. (3).

this range lose their energy while the energy is gained by the lower frequency spectral components at $f < 20$ kHz. It is in this region that we observe strong quasicoherent fluctuations in the L mode. These long wavelength fluctuations are suppressed in the H mode by the E_r shear as discussed in [14]. The $f \sim 40$ kHz feature in the H mode spectrum is indicative of the spectral region of underlying linear instability driving turbulence in the L mode. The linear growth rate γ_k [Eq. (3)], is shown in Fig. 2(d). This growth rate has a positive maximum at $f \sim$ (30–40) kHz in both the H and the L mode (unstable range). This correlates with the observation of the H mode spectral peak at $f \sim 40$ kHz. We may speculate that when the nonlinear spectral transfer is high in the L mode, energy is transferred from the unstable region both up and down the spectrum. The inverse cascade leads to the formation of quasicoherent structures. When the level of the three-wave interactions is reduced in the H mode, the spectral energy is peaked at the frequency of the linear instability at $f \sim 40$ kHz. Since the free energy for this linear instability (pressure gradient) is increased across the transition from the L to the H mode (more peaked density profile [14]), one would expect a linear growth rate to increase in this spectral region. This expectation correlates well with the observed increase in the fluctuation level at $f \sim 40$ kHz seen in Fig. 2(b) and also with our estimation of the linear growth rate shown in Fig. 2(d).

In Fig. 2(b) we show that the L mode spectrum obeys the power law fit of $P(\phi\phi^*) \sim f^{-\alpha}$, where $\alpha \approx 6$. This power law holds over 3 decades in the L mode spectrum and is observed in all the spectra in which the low frequency condensate is present. Since for large k the

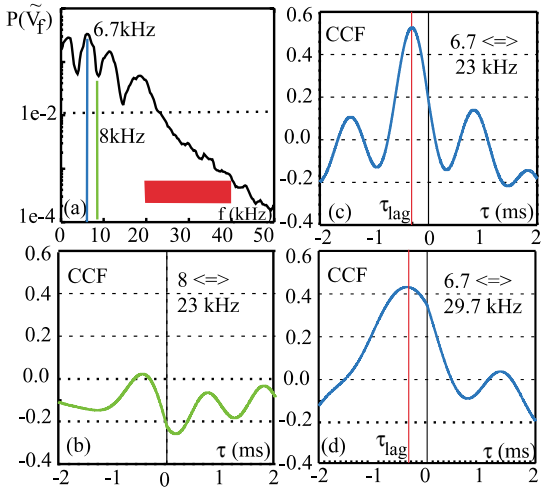

FIG. 3 (color online). (a) $\tilde{V}_f$ power spectrum. Cross-correlation functions between different spectral components: (b) $f = 8$ kHz and $f = 23$ kHz; (c) $f = 6.7$ kHz and $f = 23$ kHz; (d) $f = 6.7$ kHz and $f = 29.7$ kHz.

spectral energy is $W_k \sim k^2 P_k$ [3], the observed scaling $W \sim k^{-4}$ agrees with the theoretically expected scalings of $W \sim k^{-4}$ [3] and $P(\phi\phi^*) \sim k^{-6}$ [20].

From results of Fig. 2 it is not clear whether the spectral energy flows from the unstable region into broadband turbulence or directly into coherent structures. To investigate this, we use the amplitude correlation technique [10] which allows a better frequency resolution. Figure 3 shows cross-correlation functions (CCFs) between different components of the spectrum. Shown in Figs. 3(c) and 3(d) are the CCFs between a coherent structure at $f = 6.7$ kHz and the frequencies $f = 23$ kHz and $f = 29.7$ kHz of the unstable range. Maxima of both CCFs are high (≥ 0.4) and both maxima are observed at negative time lags. This means that the amplitude of the low frequency component lags with respect to the higher frequency one, which is interpreted as the spectral energy flow from the higher frequency to the low frequency band [10]. Note that the frequencies with high correlation satisfy a matching rule for three-wave interactions, $f = f_1 + f_2$. We identify up to six frequencies in the spectral range of $f = (20–40)$ kHz which satisfy this rule for $f = 6.7$ kHz and whose CCF maxima with this structure are higher than 0.4. This is not the case, however, for a local minimum in the spectrum at $f = 8$ kHz as seen in Fig. 3(b). The CCF maxima of this frequency with spectral components in the unstable range never exceed 0.4. Thus we may conclude that the spectral energy flows mostly into coherent structures.

Summarizing, we report the first experimental evidence of the inverse energy cascade which leads to the generation of large coherent structures and broad turbulent spectra. Many of the observations reported here agree well with the early theoretical results on the quasi-two-dimensional turbulence, including the spectral condensation, generation of zonal flows, and the power law k^{-6} spectra [3,5,20]. We believe that the agreement is largely due to the fact that in the reported experiments the polarization drift nonlinearity dominates due to the large ion gyroradius and high collisionality thus making the Hasegawa-Mima model of turbulence [8] a good approximation in our conditions.

The authors thank W. M. Solomon for useful discussions.

*Electronic address: hua.xia@anu.edu.au
†Electronic address: Michael.Shats@anu.edu.au

[1] P. C. Liewer, Nucl. Fusion **25**, 543 (1985).
[2] R. H. Kraichnan, Phys. Fluids **10**, 1417 (1967).
[3] A. Hasegawa *et al.*, Phys. Fluids **22**, 2122 (1979).
[4] W. Horton and Y. H. Ychikawa, *Chaos and Structures in Nonlinear Plasmas* (World Scientific, Singapore, 1996).
[5] A. Hasegawa and M. Wakatani, Phys. Rev. Lett. **59**, 1581 (1987).
[6] Ch. P. Ritz and E. J. Powers, Physica (Amsterdam) **20D**, 320 (1986).
[7] Ch. P. Ritz *et al.*, Phys. Fluids B **1**, 153 (1989).
[8] A. Hasegawa and K. Mima, Phys. Fluids **21**, 87 (1978).
[9] J. S. Kim *et al.*, Phys. Rev. Lett. **79**, 841 (1997).
[10] F. J. Crossley *et al.*. Plasma Phys. Controlled Fusion **34**, 235 (1992).
[11] S. M. Hamberger *et al.*, Fusion Technol. **17**, 123 (1990).
[12] M. G. Shats and W. M. Solomon, Phys. Rev. Lett. **88**, 045001 (2002).
[13] M. G. Shats and W. M. Solomon, New J. Phys. **4**, 30 (2002).
[14] M. G. Shats, Plasma Phys. Controlled Fusion **41**, 1357 (1999).
[15] W. Horton, Phys. Rev. Lett. **37**, 1269 (1976).
[16] P. Terry and W. Horton, Phys. Fluids **25**, 491 (1982).
[17] D. Newman *et al.*, Phys. Fluids B **5**, 1140 (1993).
[18] J. S. Kim *et al.*, Phys. Plasmas **3**, 3998 (1996).
[19] M. G. Shats *et al.*, Phys. Rev. Lett. **90**, 125002 (2003).
[20] D. Fyfe and D. Montgomery, Phys. Fluids **22**, 246 (1979).